

Article

# Effects of Experimental Parameters on the Extraction of Silica and Carbonation of Blast Furnace Slag at Atmospheric Pressure in Low-Concentration Acetic Acid

Kyungsun Song, Sangwon Park, Wonbaek Kim \*, Chi Wan Jeon and Ji-Whan Ahn

Climate Change Mitigation and Sustainability Division, Korea Institute of Geoscience & Mineral Resources (KIGAM), Gwahang-no 124, Yuseong-gu, Daejeon 305-350, Korea; kssong@kigam.re.kr (K.S.); psw1231@kigam.re.kr (S.P.); jcw@kigam.re.kr (C.W.J.); ahnjw@kigam.re.kr (J.-W.A.)

\* Correspondence: wbkim@kigam.re.kr; Tel.: +82-42-868-3623

Academic Editor: Kyoungkeun Yoo

Received: 26 April 2017; Accepted: 25 May 2017; Published: 30 May 2017

**Abstract:** Blast furnace slag (BFS), a calcium-rich industrial byproduct, has been utilized since 2005 as a mineral carbonation feedstock for CO<sub>2</sub> sequestration, producing calcium carbonate precipitates. In this study, the conditions for the dissolution of Ca and Si in acetic acid, and subsequent carbonation, were elaborated. For this purpose, the retardation of the polymerization of silicon was attempted by varying the concentration of acetic acid, temperature, and leaching time. An inductively coupled plasma (ICP) analysis revealed that both the Ca and Si dissolved completely within 30 min in 5% acetic acid at room temperature. This high dissolution value can be attributed to the fact that Ca was bound to O rather than to Si, as determined by X-ray photoelectron spectroscopy (XPS). The use of CO<sub>2</sub>-absorbed monoethanolamine enabled the complete carbonation of BFS at ambient conditions without the need for a pH swing. The presence of dissolved silica was found to affect the polymorphs of the precipitated CaCO<sub>3</sub>. We believe that this process offers a simple method for manipulating the composites of products obtained by mineral carbonation diminishing the leaching residues.

**Keywords:** blast furnace slag (BFS); mineral carbonation; acetic acid; calcium carbonate; dissolved silica

## 1. Introduction

Slag is the general term for the non-metallic product resulting from the separation of a metal from its raw ore. Its chemistry and morphology vary, depending on the raw materials and the solidification process. Blast furnace slag (BFS) is one of the steelmaking slags produced at high temperatures by the blast furnace route, in which a flux (limestone or dolomite) is injected to separate the iron from silicates or other impurities in the primary materials. BFS is mainly composed of CaO (30–40%), SiO<sub>2</sub> (30–40%), Al<sub>2</sub>O<sub>3</sub> (10–20%), and MgO (5–10%), along with minor components such as FeO, Na<sub>2</sub>O, and K<sub>2</sub>O [1].

Ground BFS is generally recycled as a cementitious material for use in blended Portland cements [2]. Instead of this recycling method, the recovery of certain components from the slag has attracted the attention of industry with the goal of utilizing this industrial waste. The recycled components have been restricted to silica and alumina [1], but calcium has recently gained attention as another valuable element to be used in mineral carbonation [3].

Mineral carbonation is one technical strategy for reducing the amount of CO<sub>2</sub> emitted into the atmosphere. It is based on natural weathering reactions, wherein CO<sub>2</sub> mixes with Ca- or Mg-silicate minerals, subsequently turning into carbonated solids [4]. Slag with high amounts of Ca has been

considered as an attractive feedstock because its chemical composition is similar to that of silicate minerals, and the steel industry is a large source of anthropogenic CO<sub>2</sub> emissions [5].

Most studies into the mineral carbonation of slag have focused on selective Ca dissolution and the production of relatively pure CaCO<sub>3</sub>. Other elements, including Si, were regarded as being impurities [6–8]. Silica polymerization is the main drawback affecting mineral carbonation using an acid-leaching process, because the formation of silica gel makes the solid-liquid separation challenging. Therefore, for the selective Ca leaching from BFS with a high Si content, the use of temperatures higher than 50 °C was recommended for the removal of the Si in the gel state during the dissolution process [9].

However, SiO<sub>2</sub> and Al<sub>2</sub>O<sub>3</sub>, along with CaCO<sub>3</sub>, are valuable materials. Binary composition SiO<sub>2</sub>-Al<sub>2</sub>O<sub>3</sub> has traditionally been used in the ceramics industry [10]. In addition to these applications, they have also been used as important additives in the polymer industry in either a discrete or mixed state (e.g., as inorganic fillers) [11]. The combination of CaCO<sub>3</sub> and SiO<sub>2</sub> (CaCO<sub>3</sub>-SiO<sub>2</sub> composite) has been suggested as being an ideal alternative to SiO<sub>2</sub> for the strengthening of silicon rubber [12]. Moreover, recent studies have shown that mineralization of alkaline-earth carbonates in silica-rich media leads to fascinating and intricate nanoparticle-based silica-carbonate composites referred to as “biomorphs” [13,14]. These processes are driven by pH-oscillation despite the absence of organic matters.

The solubility or crystallization of silica depends on the environment of the solution but it is generally known that its gelation is accelerated under conditions of high pH, high ionic strength, or high temperature in the acidic solution below pH 9 [15]. In an acidic solution, amorphous silica with the highest solubility is known to become monomer silicic acid, Si(OH)<sub>4</sub>. At high concentrations of dissolved silica (more than 17 mmol/L as SiO<sub>2</sub>), it can also be aged to amorphous silica, in the form of a colloid, a silica gel, or a filterable precipitate. However, a notable point is that a supersaturated silica solution can be kept in the liquid state for a relatively long duration by delaying its aggregation [16].

In the present study, we focused on the maximum recovery of not only Ca, but also Si simultaneously from BFS in the acid leaching process by preventing the silica aggregation. The aim of this study was to suggest a route for controlling the silica aggregation in the mineral carbonation of BFS to prepare silica (or calcium carbonate) compounds diminishing the leaching residues. Acetic acid (pK<sub>a</sub> of 4.76) was tested as a mild acid, with the anticipation that it could aid the carbonation without a separate pH-swing process. The phases of the calcium carbonate produced by this method were compared to determine whether they contained dissolved silica. The purity and phase of the silica were studied after being obtained through post-separation from the leachate. To prevent the inclusion of other external cations (e.g., Na from the NaOH used for the neutralization), representative amines (ammonia and monoethanolamine (MEA)) for CO<sub>2</sub> sorption were employed for the carbonation process.

## 2. Materials and Methods

### 2.1. Material Characterization

The granulated BFS was obtained from Pohang Steel Industry, Pohang, Korea. The sample was ground to a powder with particle sizes ranging from 75 to 300 μm. The chemical compositions and structures of the crystalline minerals were examined by X-ray fluorescence spectrometry (XRF) (MXF-2399, Shimadzu, Kyoto, Japan) and X-ray diffraction (XRD) (X'pert MPD, Philips Analytical, Eindhoven, The Netherlands), respectively. XRD analysis of the reaction products was carried out from 10° to 65° using Cu Kα radiation at 40 kV, 30 mA, and a scan speed of 0.04°/s. In contrast, BFS samples were examined using a step-scan mode due to the low signal/noise ratio of amorphous phase: tube voltage of 45 kV, tube current of 200 mA, step width of 0.01°, and a step duration of 1 s. X-ray photoelectron spectroscopy (XPS; K-alpha, Thermo Scientific Inc., Waltham, MA, USA) was employed to identify the bonding states of the Ca and Si elements. The binding energies were calibrated based on the contaminant hydrocarbon C1s peak at 284.8 eV. Reference samples (CaSiO<sub>3</sub>, SiO<sub>2</sub>, CaOH, and CaO) were used to determine the bonding energies of Ca, Si, and O. These reference samples were purchased from Sigma-Aldrich (ACS grade). The functional group composition of BFS was examined

using Fourier transform infrared spectroscopy (FT-IR, Prestige-21; Shimadzu Corp., Tokyo, Japan) coupled with ATR system (MIRacle A) with a Zn Se lens. Twenty scans were performed in the region of 400–4000  $\text{cm}^{-1}$  with a spectral resolution of 4  $\text{cm}^{-1}$  after appropriate background subtraction. The surface morphology of the carbonated composite was observed using field-emission scanning electron microscopy (FE-SEM) (S-4800, Hitachi, Tokyo, Japan) equipped with the energy dispersive X-ray spectrometry (EDX) at KBSI (Korea Basic Science Institute) in Daejeon, Korea. FE-SEM and EDX analysis system were operated at 10 and 15 kV, respectively. The samples were casted on a carbon tape and coated with a thin layer of platinum to eliminate the charging effect.

## 2.2. Leaching Experiments

For the extraction experiments, acetic acid (Sigma-Aldrich, St. Louis, MO, USA, ACS grade) was used. To compare the leaching potential, the extraction experiment was performed by dissolving BFS (10 g) in aqueous acetic acid (500 mL) of various concentrations (0–30% *v/v*, volume/volume percent) at 30 °C for 1 h. The exothermic nature of the BFS dissolution into acetic acid immediately caused the solution temperature to rise by 3 °C, and 30 °C could easily be attained depending on the room temperature. The effect of temperature on the silica leaching was examined in 5% (*v/v*) acetic acid at fixed temperatures (10 °C, 20 °C, and 30 °C). All of the leaching experiments were performed in a 1-L three-neck double-jacketed Pyrex glass reactor. A mechanical stirrer (WiseStir<sup>®</sup> HT120DX, Daihan Scientific Co. Ltd., Wonju, Korea) was installed at the center of the reactor and was used to mix the slurry at 500 rpm. The temperature of the reactor was maintained using an external circulating water bath (RW-1025, JEIL TECH, Daejeon, Korea). The suspension was sampled (20-mL samples) at predetermined intervals for 2 h from the start of the reaction. The filtration was performed using a 0.2- $\mu\text{m}$  membrane filter (mixed cellulose ester, Advantec Co., Tokyo, Japan). A 1-mL filtered sample was acidified with instrument-grade  $\text{HNO}_3$  to 5% (*v/v*) to determine the concentrations of five major elements (Ca, Si, Mg, Fe, and Al) using inductively-coupled plasma optical emission spectrometry (ICP-OES; Optima 5300DV, PerkinElmer, Waltham, MA, USA). The pH and temperature of the mixture were monitored by a pH meter (Orion 410A, Thermo Scientific, Waltham, MA, USA). All the experiments were performed in duplicate, and the variations between the results were found to be <7%.

## 2.3. Separation of Silica

The temperature had a significant influence on the stability of the dissolved silica in the leached solution. Gelation was not observed for seven days in the leached solution of 5% acetic acid, when stored in a refrigerator (at 2 °C). To investigate the effect of temperature on silica recovery from the leachate, the extracted solution of 5% acetic acid (before the gelation was initiated) was stirred at 30 °C, 50 °C, or 70 °C for 2 h and filtered. The gel was recovered by mechanical filtering using a 1.0- $\mu\text{m}$  membrane filter (mixed cellulose ester, Advantec Co., Tokyo, Japan), washed with deionized water (purified using a Milli-Q 18 M $\Omega$ -cm system), and then dried overnight in a vacuum at 80 °C. The composition of the gel was estimated from the differences between the concentrations of major five metals in the leachate before and after gelation. The dried gel formed coarse particles. The stoichiometry of the components was assumed from the depth profiles by using an XPS etching technique (K-alpha, Thermo Scientific Inc., West Palm Beach, FL, USA). The depth profiles were obtained using an Ar-ion beam with the following experimental parameters: ion energy of 1 keV, ion current of 2.0  $\mu\text{A}$ , etching rate of 0.15 nm/s, and area of 2  $\times$  2  $\text{mm}^2$ . The granules were ground to a powder in a mortar, which was then analyzed by X-ray diffraction (XRD). The powdered sample was sintered by heat-treating at 1100 °C for 3 h, after which the phase transformation was examined.

## 2.4. Carbonation Experiments

The carbonation experiments were performed via two pathways using a leached solution in 5% (*v/v*) acetic acid at room temperature for 30 min: One pathway was to carbonate after removing the silica-rich gel, while the other was to carbonate all of the leachates prior to the gel formation.

The carbonation reactions were all performed at ambient temperature and pressure using ammonium carbonate (Sigma-Aldrich, ACS grade), ammonium bicarbonate (Sigma-Aldrich, ACS grade), and CO<sub>2</sub>-loaded MEA (1 M). The CO<sub>2</sub>-loaded MEA solution was prepared as described in a previous study [17]. A CO<sub>2</sub> analyzer (Multi-Master, Sensoronic Co., Ltd., Bucheon, Korea) was used to determine the relative amount of absorbed CO<sub>2</sub>. The solutions (200 mL) prepared via the two pathways were gently mixed with the CO<sub>2</sub>-bearing solution (200 mL) in a conical 600-mL flask. In the case of the ammonium (bi) carbonate, absorbed CO<sub>2</sub> gas was reverse-ejected and failed to carbonate the BFS. In contrast, in the case of the CO<sub>2</sub>-loaded MEA, the formation of white particles was detected upon mixing. Morphological changes in the particles were examined after the solution had been stirred for 3 h or 24 h using a magnetic stirring bar rotating at 200 rpm. After stirring for the required duration, the as-formed particles were filtered using a 0.2- $\mu$ m membrane filter (mixed cellulose ester, ADVANTEC). The composite of the carbonated products was assumed based on the difference between the concentrations of the five major metals in the solutions before and after the carbonation reaction. The filtered solid samples were washed with deionized water purified using a Milli-Q 18 M $\Omega$ -cm system (Millipore Corp., Milford, MA, USA) and then dried overnight in vacuum at 80 °C. Phases of samples were then examined by XRD.

### 3. Results and Discussion

#### 3.1. Characterization of BFS

The XRF and XRD analyses showed that the BFS was mainly composed of Ca (43.4% as CaO), Si (37.7% as SiO<sub>2</sub>), and Al (13.4% as Al<sub>2</sub>O<sub>3</sub>) in amorphous phases (Table 1 and Figure 1). In addition to the amorphous phase, a small crystalline peak was also detected at around 29°. We could not positively index the crystalline material; one reason being that it would be a major peak of a compound of unknown composition. The granulated BFS is usually in the amorphous phase because of the short-duration water cooling. The chemical or structural characteristics are within the typical range for BFS.

**Table 1.** Chemical composition of blast furnace slag.

Chemical Composition (wt %)									
CaO	SiO <sub>2</sub>	Al <sub>2</sub> O <sub>3</sub>	MgO	Fe <sub>2</sub> O <sub>3</sub>	Ti <sub>2</sub> O	K <sub>2</sub> O	MnO	Na <sub>2</sub> O	P <sub>2</sub> O <sub>5</sub>
43.4	37.7	13.4	3.82	1.33	0.33	0.24	0.23	0.18	0.02

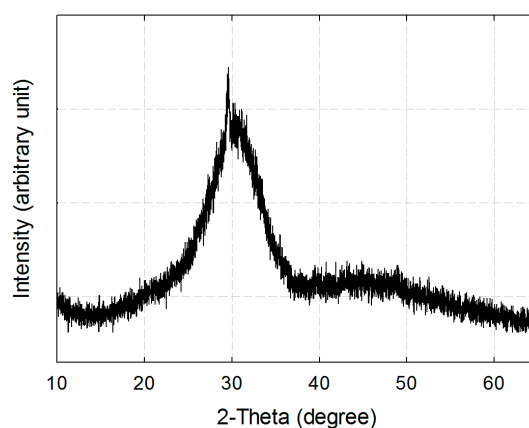


**Figure 1.** X-ray diffractogram of blast furnace slag analyzed by a step-scan mode.

For a detailed analysis of BFS structure, IR and XPS measurements were performed. As shown in Figure 2, three distinct absorption bands are observed: strong two at near 900 cm<sup>-1</sup> and 450 cm<sup>-1</sup> and small one near 700 cm<sup>-1</sup>. The bands at around 900 cm<sup>-1</sup> and 700 cm<sup>-1</sup> are the characteristic peaks

assignable to asymmetric and symmetric stretching vibrations of Si-O. The band around  $450\text{ cm}^{-1}$  is assigned to the deformation of  $\text{MO}_4$  tetrahedra ( $\text{M} = \text{Si}, \text{Al}, \text{Mg}, \text{etc.}$ ) [18,19].

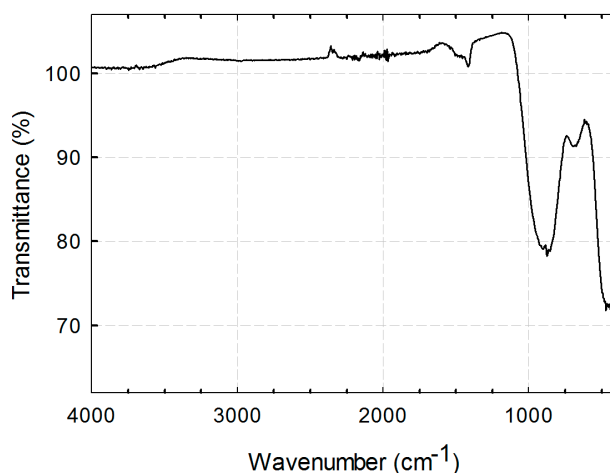


Figure 2. FT-IR spectrum of blast furnace slag.

The bonding state of the elements in BFS can be an important factor when slag is dissolved in a weak acetic acid aqueous solution. The Ca–O bond is reported to be more liable to dissolve than the Ca–Si–O bond in the acid leaching of BFS [7]. In this study, XPS analysis was employed to investigate the binding state of Ca and Si using reference samples of  $\text{CaSiO}_3$ ,  $\text{SiO}_2$ ,  $\text{CaOH}$ , and  $\text{CaO}$ .

As shown in Figure 3a, the binding energy of Ca (347.5 eV) better matches that of Ca in  $\text{CaOH}$  (347.2 eV) and  $\text{CaO}$  (347.2 eV) than that of Ca in  $\text{CaSiO}_3$  (345.6 eV). This suggests that Ca is likely to bind to O rather than Si; i.e., the lime and calcium hydroxide phases. In the case of Si, the binding energy of Si is 102.2 eV, which is comparable to the value of non-crystalline and non-stoichiometric Si oxide (Figure 3b) [20,21]. The oxide forms of Ca and Si can also be confirmed by the O 1s photoelectron peak of the slag (Figure 3c). When we compare the  $\text{CaO}$  and  $\text{CaOH}$  peaks, the slag peak is clearly broader, possibly due to the native heterogeneity of the slag. Based on the XPS results, calcium and silica are likely to bond as (hydr-) oxides and bonding between metals scarcely exists.

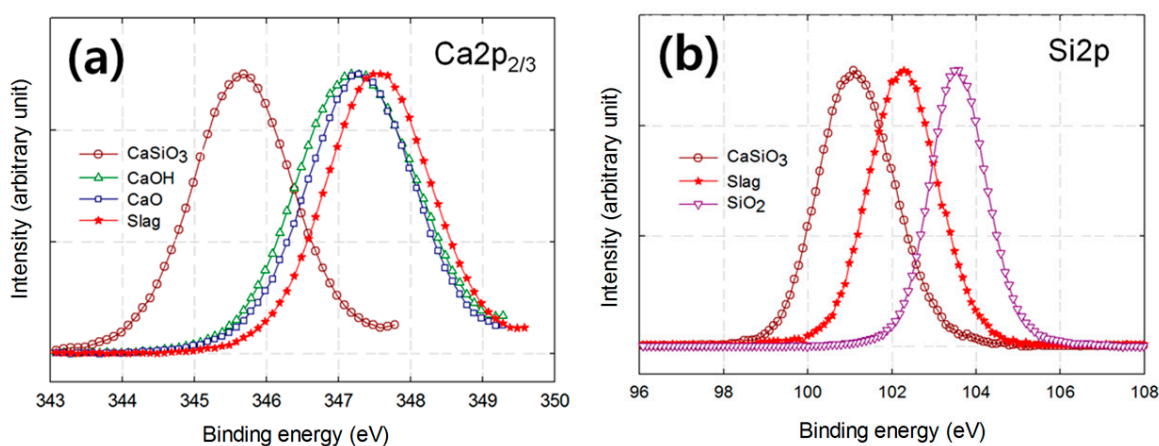


Figure 3. Cont.

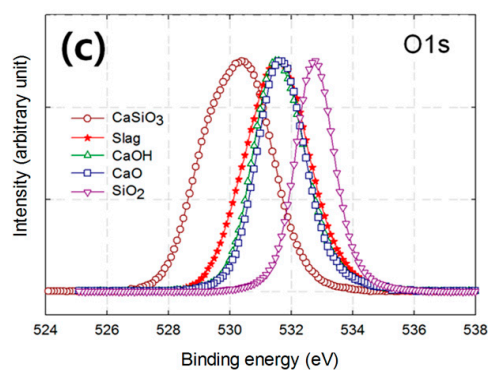


Figure 3. (a) Ca 2p; (b) Si 2p; and (c) O 1s XPS spectra of blast furnace slag.

### 3.2. Optimization of Leaching Parameters

The results of previous studies of the dissolution of slag using acetic acid [6,8,9] can be summarized as follows:

1. The dissolution process is so fast that it completes in a few minutes with an exothermic nature.
2. The solubility of slag, and especially the extraction of Ca, decreased with increasing temperature.
3. The removal of silicon was much easier at higher temperatures of 70 °C and 80 °C.
4. A high concentration of acetic acid (i.e., 33 wt %) and a temperature of 70 °C were found to be the optimal conditions for the removal of the silicon-rich gel and the extraction of Ca.

In this study, we focused on the simultaneous recovery of both calcium and silicon using less acetic acid and lower temperature without a pH swing. To this end, it is important to determine the optimum conditions under which the lowest concentration of acetic acid is required to keep the solution supersaturated with dissolved silica for as long as possible.

In the first instance, the effect of the concentration of the acetic acid was investigated by varying the concentration (0%, 2%, 5%, 10%, 20%, and 30% *v/v*) at 30 °C. Figure 4 shows the effect of acetic acid concentration on the extraction of the major elements. The BFS dissolved easily in a low concentration of acetic acid. An acetic acid solution of 2% could dissolve about 70% of the Ca and all the Ca dissolved completely when the concentration exceeded 5%. This means that a maximum of 2.5 mL of acetic acid would be required to extract all the Ca from 1 g of BFS. This is the minimum amount of acetic acid required to extract Ca from 1 g of BFS. This value is about half the amount (6–7 mL) previously reported by Teir et al. [8]. Based on the amount of leached Ca, the capacity for CO<sub>2</sub> sequestration would be 0.43 kg of CO<sub>2</sub>/kg of BFS. This higher value may be attributable to the Ca-O bond shown in the XPS results. One notable result is that the amount of leached Si decreases once the acetic acid concentration exceeds 20%. This can be ascribed to the fact that the increased ionic strength would accelerate the silica aggregation [15].

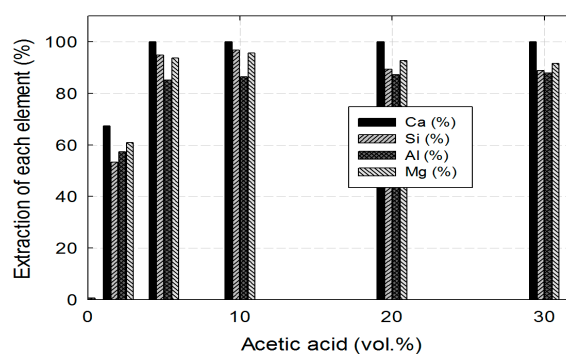
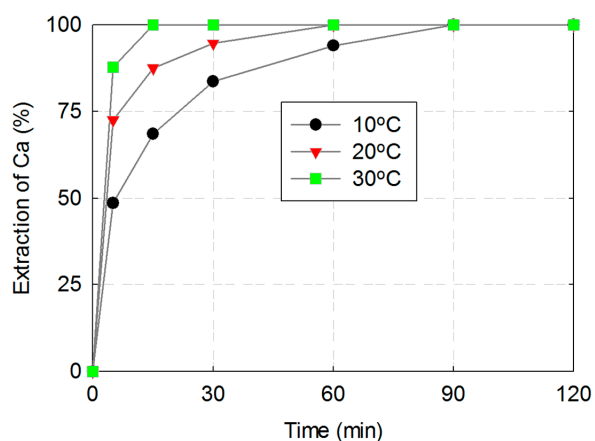
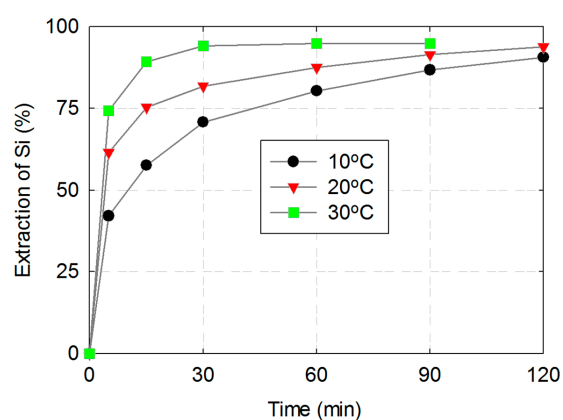


Figure 4. Dissolution of blast furnace slag at 30 °C for 60 min in various concentrations of acetic acid.

As shown in Figure 4, an aqueous solution of 5% acetic acid was the optimal concentration for extraction from a batch of slag. The temperature is a crucial factor affecting both the calcium extraction and silica aggregation. Therefore, we investigated the effect of temperature on the dissolution of Ca and Si at 10 °C, 20 °C, and 30 °C using an aqueous solution of 5% acetic acid for 2 h. The dissolution rates of the Ca and Si both increased with temperature. It was found that the calcium dissolved completely within 90 min at all temperatures (Figure 5). Meanwhile, the silica gelation was accelerated at 30 °C, making the filtering at 2 h difficult (Figure 6). Apparently, the rate of silica dissolution increased with the temperature to some extent but an excessive temperature has an adverse effect by promoting the silica aggregation.



**Figure 5.** Ca dissolution from blast furnace slag using an aqueous solution of 5% acetic acid.



**Figure 6.** Si dissolution from blast furnace slag using aqueous solution of 5% acetic acid.

### 3.3. Post-Leaching Separation of Silica

To obtain relatively pure calcium carbonate from BFS, highly-concentrated acetic acid and a high temperature are required to remove impurities, mainly silica, in the leaching process. However, in this study, we set up the dissolution condition so that the leachate can contain the maximum amount of dissolved silica.

The soluble form of silica presents as  $\text{Si}(\text{OH})_4$ , monomeric silica, in an acidic solution. Silica aggregation is known to induce gelation by polymerizing the discrete silica particles. Once the viscose silica gel is formed, a reverse reaction rarely occurs even in the presence of large amounts of water.

The simple equation for silica polymerization is as follows:



The zero point of charge ( $\text{pH}_{\text{zpc}}$ ) of colloidal silica is around 2, and the aggregation rate is the minimum near pH 2. Above this pH (especially above pH 5), the colloidal silica is negatively charged and the aggregation increases. In addition to the pH, high temperatures are generally recognized as being another significant factor increasing the silica aggregation.

The effect of temperature on the silica aggregation was investigated to determine the optimum conditions under which as much dissolved silica as possible can be separated. After leaching using 5% acetic acid solution at room temperature, the solution was stirred at various temperatures (30 °C, 50 °C and 70 °C) to examine the aggregating behavior of the dissolved silica.

The gel was detected after 1 h of stirring at 30 °C, but it formed immediately when the temperature was increased to 50 °C or 70 °C. Regardless of the temperature, the hydrated gel was white and formed coarse (glass-like) particles after drying (Figure 7). However, the chemical components of the gel differed depending on the temperature (Figure 8). The amount of silica and aluminum recovered from the leachate into the gel increased as with the temperature. The amount of iron included in the gel was not affected by the temperature. Up to 93% Si and 66% Al were incorporated into the gel from the leachate at 70 °C. The gel was assumed to be composed of roughly 80% (*w/w*)  $\text{SiO}_2$  and 20% (*w/w*)  $\text{Al}_2\text{O}_3$ . The silica-rich gel formed during the acid extraction of BFS was reported to also include considerable amounts of calcium, in addition to the silicon [8]. One noticeable result is that there is no calcium nor magnesium in the gel obtained after the acid leaching process. This observation implies that the acid extraction of BFS following subsequent heating to 70 °C may be more suitable for carbonation requiring the recovery of larger amounts of calcium.

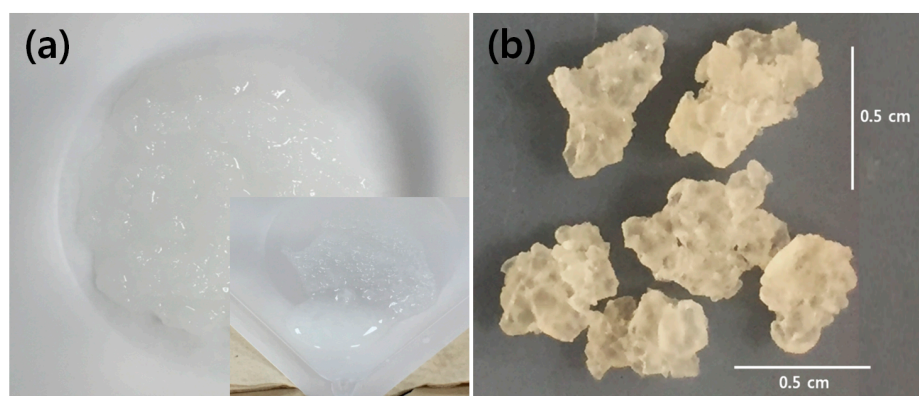


**Figure 7.** (a) Hydrated gel formed in solution extracted with 5% acetic acid, and (b) the dried state after mechanical filtering of (a).

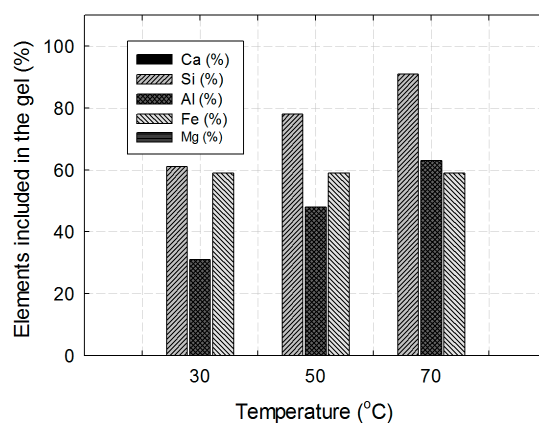


**Figure 8.** Relative amounts of elements included in the gel.

As shown in Figure 7b, the surface of the gel appears very coarse. Therefore, we obtained a depth profile using an XPS etching technique to examine the extent of the homogeneous distribution of the major elements depending on the depth in the gel. As shown in Figure 9, as the distance from the surface increased, only two elements, silicon and oxygen, were detected. The stoichiometry can be assumed to be two, as  $\text{SiO}_2$ . The other elements could not be quantified because their amounts fell below the detection limit of 5% (at. %).

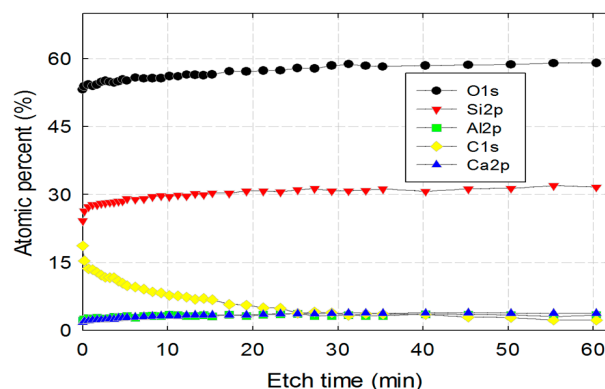


Figure 9. Depth profile of the gel formed from leachate at 70 °C.

It is well known that amorphous phase  $\text{SiO}_2$  turns into crystalline-phase cristoballite, a ceramic material, by sintering [22]. To examine the possibility of this silica-rich gel turning into cristoballite, it was powdered and calcined at 1100 °C for 3 h. As shown in Figure 10, the uncalcined amorphous powders turned into crystalline cristobalite with a small amount of mullite ( $\text{Al}_6\text{Si}_2\text{O}_{13}$ ). Mullite is a precious material with a high melting point and low thermal expansion, and is known to be formed in an  $\text{Al}_2\text{O}_3$ - $\text{SiO}_2$  system with a narrow composition range (10–50 mol %  $\text{Al}_2\text{O}_3$ ) [10].

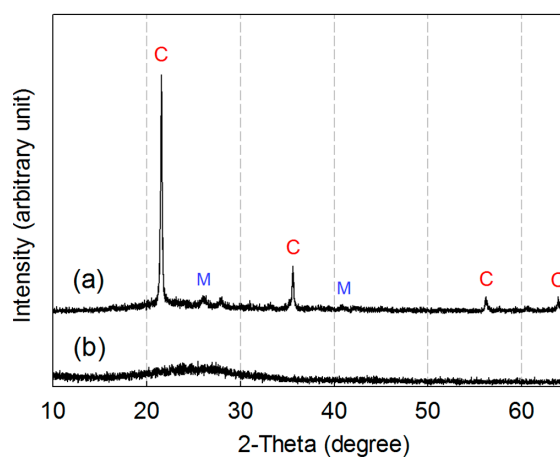
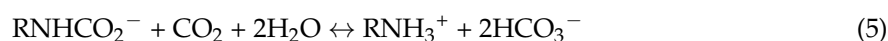


Figure 10. XRD patterns of (a) product sintered at 1100 °C for 3 h with (b) powdered gel obtained from leachate. C and M represent cristobalite and mullite, respectively.

### 3.4. Carbonation of BFS

In general, carbonation using BFS consists of acid dissolution and a pH swing with an alkaline agent (i.e., NaOH) or high-pressure  $\text{CO}_2$  gas. However, we tried to attain the carbonation of BFS without a pH swing step at atmospheric pressure by using a  $\text{CO}_2$ -absorbed amine solution. Ammonia is a typical amine used in the post-combustion  $\text{CO}_2$  capture process. We performed a preliminary feasibility test on the carbonation without a separate pH swing process by using ammonium carbonate

and bicarbonate. However, the carbonation failed to proceed and CO<sub>2</sub> gas was ejected as the leached solution was dropped. Given this result, we deliberated another CO<sub>2</sub>-embraced amine capable of acting as a buffer to some extent. Once the CO<sub>2</sub> gas reacts with the amine solution, it is converted to a carbonate, bicarbonate, or carbamate. The main reactions can be summarized as follows:



As shown in above equations, a proton introduced from the acid-leached solution would be neutralized mainly with anions, such as RNHCO<sub>2</sub><sup>-</sup>, HCO<sub>3</sub><sup>-</sup>, and CO<sub>3</sub><sup>2-</sup>. Here, R corresponds to H in ammonia. In the case of ammonia, the buffer capacity of the (bi) carbonate would be expected to be less such that a reverse reaction of Equation (3) could easily occur if the proton is introduced by the acetic acid, even if in very small amounts. The buffer capacity can be increased thanks to the electronegative nitrogen in one amine group, but its effect would be weak. In contrast, R corresponds to HOCH<sub>2</sub>CH<sub>2</sub> in the case of MEA (HOCH<sub>2</sub>CH<sub>2</sub>NH<sub>2</sub>), another typical amine used in the CO<sub>2</sub> capture process. This offers some advantages in that it contains a hydroxyl group that is protonated, in addition to an amine group. Actually, the protonation of the hydroxyl group of MEA has been observed as a result of the addition of acid [23]. The initial pH of the MEA solution was 12.5 and decreased as the loaded CO<sub>2</sub> amount increased. Therefore, we used the CO<sub>2</sub>-loaded MEA (pH of 10.2) solution in which the dominant species would be carbamate and the free MEA would remain at about 50%.

To obtain relatively pure calcium carbonate precipitates, we performed carbonation with a CO<sub>2</sub>-loaded MEA solution using a solution from which 93% Si and 66% Al had been removed by gelation as described in Section 3.3. The carbonation yield was almost 100% because the concentration of calcium in the filtered solution after the carbonation reaction was almost zero, as determined by ICP-OES analyses. The precipitated calcium carbonate was composed of 85 wt % Ca with 6 wt % Mg, 6 wt % Al, and 3 wt % Si. The carbonation product was white, unlike the mother slag. This improvement in the whiteness can be confirmed by comparing photographs of the slag and the carbonated product (Figure 11).



**Figure 11.** (a) The blast furnace slag as-received and (b) carbonated product obtained after removing silica-rich gel.

Calcium carbonate exists in three crystalline phases, namely, vaterite, aragonite, and calcite. Calcite is the most stable phase, and the metastable phases (aragonite and vaterite) turn into calcite as a result of

a solvent-mediated transformation in an aqueous solution [24]. To check whether this transformation occurred, the stirring time was extended to 24 h. We noted that the crystal structure of the carbonated product varied depending on the stirring time (Figure 12). When the stirring time was short (3 h), all of the crystalline phases (vaterite, calcite, and aragonite) were present, though vaterite was the dominant phase. On the other hand, calcite was the dominant phase with only a small amount of vaterite after stirring for 24 h. This observation agrees with previously obtained results, in which vaterite prevailed initially, but was then transformed to calcite during the carbonation reaction using MEA media [25].

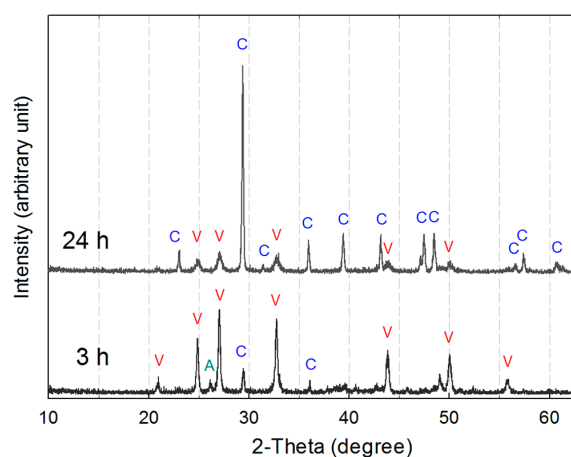


**Figure 12.** XRD patterns of carbonated product obtained after removing silica-rich gel. C, V, and A represent calcite, vaterite, and aragonite, respectively.

To investigate the effect of the dissolved silica on the produced calcium carbonate, we conducted the carbonation reaction using the as-leached solution without the removal of silica-rich gel. Furthermore, we intended to test the possibility of preparing a composite of  $\text{CaCO}_3\text{-SiO}_2$  using this solution.

The phases of the carbonated products were very different from that which we obtained after removing the silica-rich gel. XRD observations show that the carbonated product was exclusively calcite, regardless of the stirring period (Figure 13). This result implies that the dissolved elements (especially silica) may have a significant influence on the polymorph of calcium carbonate. A similar calcite-stabilizing effect of the dissolved silica was previously observed [26]. This was ascribed to the fact that dissolved silica either decreases the energy barrier for the nucleation of calcite or inhibits vaterite formation by providing nucleation sites.

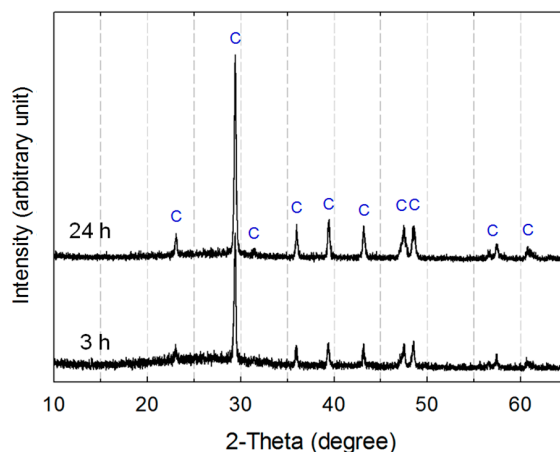


**Figure 13.** XRD patterns of the carbonated product in the presence of dissolved silica.

Figure 14 shows FE-SEM images of the composite particles. Those composite particles are in contact with the SiO<sub>2</sub> nanoparticles attached to the surface of calcium carbonates of an aggregated and rather unspecific structure. The scattering and distribution of SiO<sub>2</sub> nanoparticles on the surface can be confirmed by EDX mapping images shown in Figure 15. This is comparable to the observations made in a previous study [24]. They synthesized CaCO<sub>3</sub>-SiO<sub>2</sub> composite particles using CaCO<sub>3</sub> and SiO<sub>2</sub> powders, and observed that the SiO<sub>2</sub> particles are scattered around the CaCO<sub>3</sub> particles. This demonstrates that an in situ composite of CaCO<sub>3</sub>-SiO<sub>2</sub> may be possible through the carbonation of an as-leached solution.

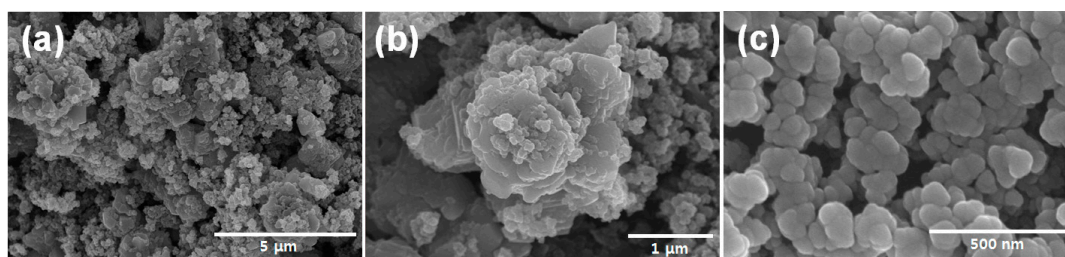


**Figure 14.** FE-SEM images of composite particles of carbonated product: (a) at low magnification; (b) at high magnification; and (c) clustered SiO<sub>2</sub> nanoparticles.

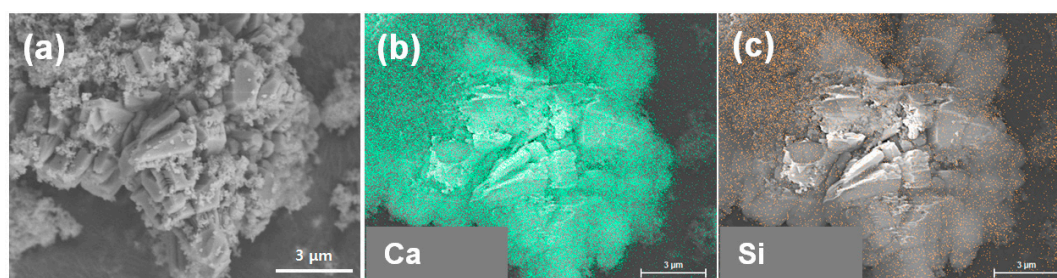


**Figure 15.** (a) FE-SEM image of composite particles, and the corresponding EDX mapping images of (b) Ca and (c) Si.

#### 4. Conclusions

Blast furnace slag (BFS) has been utilized for mineral carbonation due to its high calcium content (30–40% as CaO). However, the other major constituent element, silicon (30–40% as SiO<sub>2</sub>), has been treated as an impurity or a hindrance to the preparation of CaCO<sub>3</sub> or a CO<sub>2</sub> sequestration process because of its aggregating nature. In this study, we optimized the experimental parameters, including the temperature, acetic acid concentration, and reaction period to dissolve not only the calcium, but also the silicon in the BFS by retarding the polymerization of silica in acetic-acid aqueous solution.

The BFS exhibited a high solubility in 5% acetic acid at room temperature, with both the Ca and Si completely dissolving within 30 min. Based on the amount of extracted Ca, the CO<sub>2</sub> sequestration capacity could reach as much as 0.43 kg of CO<sub>2</sub>/kg BFS. The high dissolution value can possibly be attributed to the fact that the Ca is bound to O rather than Si, as determined by X-ray photoelectron spectroscopy (XPS). In addition, the carbonation of BFS at atmospheric temperature and pressure could be realized using CO<sub>2</sub>-absorbed monoethanolamine with an acetic acid-leached solution. The carbonation was performed along either of two pathways to evaluate the effect of dissolved silica on the carbonate products, i.e., with or without dissolved silica.

In the case of carbonation without dissolved silica, silica removal was attempted by varying the temperature of the leached solution and 93% Si could be removed as glass-like silica-rich gel at 70 °C. An X-ray diffraction study indicated that the gel was amorphous and transformed mainly to cristoballite by sintering at 1100 °C. Meanwhile, the carbonation product obtained after removing the

Si was initially vaterite, which transformed to the more stable calcite as a result of a solvent-mediated transformation. In contrast, the carbonation with the dissolved silica produced micro-sized calcite particles with amorphous SiO<sub>2</sub> nanoparticles attached to the surface of rhombohedral-shaped CaCO<sub>3</sub>, demonstrating the effect of the dissolved silica on the stabilization of the calcite phase. Thus, the method developed herein can be used to control the composites of the carbonated products diminishing the leaching residues in the mineral carbonation of BFS.

**Acknowledgments:** This research was supported by the Basic Research Project of the Korea Institute of Geoscience and Mineral Resources (KIGAM) funded by the Ministry of Science, ICT and Future Planning. This work was also supported by the Korea Institute of Energy Technology Evaluation and Planning (KETEP) through the Energy Technology Innovation (ETI) program (2013T100100021).

**Author Contributions:** Kyungsun Song and Wonbaek Kim designed and managed the study; Sangwon Park and Chi Wan Jeon performed carbonation experiments and analyzed the data; Ji-Whan Ahn conceptualized and interpreted data.

**Conflicts of Interest:** The authors declare no conflicts of interest.

## References

1. Seggiani, M.; Vitolo, S. Recovery of silica gel from blast furnace slag. *Resour. Conserv. Recycl.* **2003**, *40*, 71–80. [[CrossRef](#)]
2. Osborne, G.J. Durability of portland blast-furnace slag cement concrete. *Cem. Concr. Compos.* **1999**, *21*, 11–21. [[CrossRef](#)]
3. Eloneva, S.; Said, A.; Fogelholm, C.-J.; Zevenhoven, R. Preliminary assessment of a method utilizing carbon dioxide and steelmaking slags to produce precipitated calcium carbonate. *Appl. Energy* **2012**, *90*, 329–334. [[CrossRef](#)]
4. Seifritz, W. CO<sub>2</sub> disposal by means of silicates. *Nature* **1990**, *345*, 486. [[CrossRef](#)]
5. Huijgen, W.J.J.; Comans, R.N.J. Mineral CO<sub>2</sub> sequestration by steel slag carbonation. *Environ. Sci. Technol.* **2005**, *39*, 9676–9682. [[CrossRef](#)] [[PubMed](#)]
6. De Crom, K.; Chiang, Y.W.; Van Gerven, T.; Santos, R.M. Purification of slag-derived leachate and selective carbonation for high-quality precipitated calcium carbonate synthesis. *Chem. Eng. Res. Des.* **2015**, *104*, 180–190. [[CrossRef](#)]
7. Eloneva, S.; Teir, S.; Salminen, J.; Fogelholm, C.-J.; Zevenhoven, R. Steel converter slag as a raw material for precipitation of pure calcium carbonate. *Ind. Eng. Chem. Res.* **2008**, *47*, 7104–7111. [[CrossRef](#)]
8. Teir, S.; Eloneva, S.; Fogelholm, C.-J.; Zevenhoven, R. Dissolution of steelmaking slags in acetic acid for precipitated calcium carbonate production. *Energy* **2007**, *32*, 528–539. [[CrossRef](#)]
9. Eloneva, S.; Teir, S.; Salminen, J.; Fogelholm, C.-J.; Zevenhoven, R. Fixation of CO<sub>2</sub> by carbonating calcium derived from blast furnace slag. *Energy* **2008**, *33*, 1461–1467. [[CrossRef](#)]
10. Macdowell, J.F.; Beall, G.H. Immiscibility and crystallization in Al<sub>2</sub>O<sub>3</sub>-SiO<sub>2</sub> glasses. *J. Am. Ceram. Soc.* **1969**, *52*, 17–25. [[CrossRef](#)]
11. Razak, J.A.; Akil, H.M.; Ong, H. Effect of inorganic fillers on the flammability behavior of polypropylene composites. *J. Thermoplast. Compos. Mater.* **2007**, *20*, 195–205. [[CrossRef](#)]
12. Cui, C.; Ding, H.; Cao, L.; Chen, D. Preparation of CaCO<sub>3</sub>-SiO<sub>2</sub> composite with core-shell structure and its application in silicone rubber. *Pol. J. Chem. Technol.* **2015**, *17*, 128. [[CrossRef](#)]
13. Kellermeier, M.; Cölfen, H.; García-Ruiz, J.M. Silica biomorphs: Complex biomimetic hybrid materials from “sand and chalk”. *Eur. J. Inorg. Chem.* **2012**, *2012*, 5123–5144. [[CrossRef](#)]
14. Noorduyn, W.L.; Grinthal, A.; Mahadevan, L.; Aizenberg, J. Rationally designed complex, hierarchical microarchitectures. *Science* **2013**, *340*, 832–837. [[CrossRef](#)] [[PubMed](#)]
15. Terry, B. The acid decomposition of silicate minerals part II. Hydrometallurgical applications. *Hydrometallurgy* **1983**, *10*, 151–171. [[CrossRef](#)]
16. Kazadi, D.M.; Groot, D.R.; Steenkamp, J.D.; Pöllmann, H. Control of silica polymerisation during ferromanganese slag sulphuric acid digestion and water leaching. *Hydrometallurgy* **2016**, *166*, 214–221. [[CrossRef](#)]
17. Park, S.; Lee, M.-G.; Park, J. CO<sub>2</sub> (carbon dioxide) fixation by applying new chemical absorption-precipitation methods. *Energy* **2013**, *59*, 737–742. [[CrossRef](#)]

18. Puertas, F.; Fernández-Jiménez, A. Mineralogical and microstructural characterisation of alkali-activated fly ash/slag pastes. *Cem. Concr. Compos.* **2003**, *25*, 287–292. [[CrossRef](#)]
19. Kuwahara, Y.; Ohmichi, T.; Kamegawa, T.; Mori, K.; Yamashita, H. A novel conversion process for waste slag: Synthesis of a hydrotalcite-like compound and zeolite from blast furnace slag and evaluation of adsorption capacities. *J. Mater. Chem.* **2010**, *20*, 5052–5062. [[CrossRef](#)]
20. Li, H.; Sun, H.; Tie, X.; Xiao, X. A new method to evaluate the hydraulic activity of Al-Si materials. *Sci. China Technol. Sci.* **2008**, *51*, 113–120. [[CrossRef](#)]
21. Lehner, A.; Steinhoff, G.; Brandt, M.S.; Eickhoff, M.; Stutzmann, M. Hydrosilylation of crystalline silicon (111) and hydrogenated amorphous silicon surfaces: A comparative X-ray photoelectron spectroscopy study. *J. Appl. Phys.* **2003**, *94*, 2289–2294. [[CrossRef](#)]
22. Fang, Y.; Li, L.; Xiao, Q.; Chen, X.M. Preparation and microwave dielectric properties of cristobalite ceramics. *Ceram. Int.* **2012**, *38*, 4511–4515. [[CrossRef](#)]
23. McCann, N.; Phan, D.; Wang, X.; Conway, W.; Burns, R.; Attalla, M.; Puxty, G.; Maeder, M. Kinetics and mechanism of carbamate formation from CO<sub>2</sub> (aq), carbonate species, and monoethanolamine in aqueous solution. *J. Phys. Chem.* **2009**, *113*, 5022–5029. [[CrossRef](#)] [[PubMed](#)]
24. Wen, X.; Liu, Y.; Xu, Z.; Yang, J.; Pi, P.; Cai, Z.; Cheng, J.; Yang, Z. Mechano-chemical preparation and application of mulberry-like CaCO<sub>3</sub>/SiO<sub>2</sub> composite particles in superhydrophobic films. *Soft Mater.* **2012**, *10*, 435–448. [[CrossRef](#)]
25. Vučak, M.; Perić, J.; Pons, M.N.; Chanel, S. Morphological development in calcium carbonate precipitation by the ethanolamine process. *Powder Technol.* **1999**, *101*, 1–6. [[CrossRef](#)]
26. Lakshtanov, L.Z.; Stipp, S.L.S. Interaction between dissolved silica and calcium carbonate: 1. Spontaneous precipitation of calcium carbonate in the presence of dissolved silica. *Geochim. Cosmochim. Acta* **2010**, *74*, 2655–2664. [[CrossRef](#)]



© 2017 by the authors. Licensee MDPI, Basel, Switzerland. This article is an open access article distributed under the terms and conditions of the Creative Commons Attribution (CC BY) license (<http://creativecommons.org/licenses/by/4.0/>).